Torque Ripple Minimisation in Switched Reluctance Motors by Optimisation of Current Wave-Forms and of Teeth Shape with Copper Losses and V.A. Silicon Constraints

Jean-Yves Le Chenadec, Marc Geoffroy, Bernard Multon, Jean-Claude Mouchoux

ICEM'94 (Paris), 5-7 Sept. 1994, Vol.2, pp.559-564.

TORQUE RIPPLE MINIMISATION IN SWITCHED RELUCTANCE MOTORS BY OPTIMISATION OF CURRENT WAVE-FORMS AND OF TOOTH SHAPE WITH COPPER LOSSES AND "V.A. SILICON" CONSTRAINTS

MINIMISATION DES ONDULATIONS DE COUPLE DANS LES MOTEURS A RELUCTANCE VARIABLE A DOUBLE SAILLANCE PAR OPTIMISATION DES FORMES DE COURANT ET DES ANGLES POLAIRES AVEC CONTRAINTES DES PERTES JOULE ET DE "PUISSANCE SILICIUM"

Jean-Yves LE CHENADEC, Marc GEOFFROY, Bernard MULTON, Jean-Claude MOUCHOUX
LÉSiR URA CNRS D1375, École Normale Supérieure de Cachan
61, Avenue du Président Wilson, F 94 235 CACHAN Cédex, FAX : (1)47 40 21 99

Abstract

The main aim of this paper is the minimisation of torque ripple in a 6/4 switched reluctance motor by current waveforms and pole arc optimisation and with realistic constraints. This research is based on a magnetic structure with several sizes which remain constant : outer diameter (250 mm), stack length (150 mm), shaft diameter (42 mm) and airgap length (0.8 mm at radius). We computed, by the finite-element method, electromagnetic characteristics (torque and flux versus amperes-turns and angular position) for several stator and rotor pole arc values (5 machines called M1 to M5). Before these computations were conducted, the main sizes of each machine were optimised by a quick analytical method to minimise copper losses at low speed and with an ideal square wave current supply. Then, we determined, for each machine, the optimal current waveforms to minimise the torque ripple yoke thickness, etc...) were optimised (section 2) to maximise the average torque with a square-wave current supply and with limited copper losses (1500 W). In each case, by numerical computation, we performed an optimisation of current waveforms [8, 9] to in taking account of voltage and maximum current limitations. Maximum volts-amperes of converter (3 asymmetrical half bridges) were limited to a value corresponding to that of a typical three phase inverter which supplies classical alternative current motors (induction or permanent magnet). On this basis, we compared the 5 machines in terms of minimum torque ripple and copper losses. It appeared that the pole arc choice results from a compromise between torque ripple and copper losses.

Keywords:
Switched Reluctance Motor,
Torque Ripple,
Pole-Arc,
Motor-Converter Optimisation

1 INTRODUCTION

Switched reluctance motors [1] are used because of their high performance in terms of efficiency and their low cost. While they have been applied in some new markets, their natural torque ripple has to be reduced to permit broader applications. Over the past, some laboratories [2, 3, 4, 5, 6] have obtained results, but these results haven't taken into account the intrinsic limits of the "silicon apparent power" [7] of the converter together with the electromagnetic characteristics of the motor.

Using the example of a designed and built switched reluctance motor for an electric vehicle application [10] (Structure 6/4 with approximate ratings : maximum torque : 100 N.m and maximum power : 30 kW), we determined, with the finite-element method, natural torque characteristic arrays for this motor [11] in seven cases. Each case corresponded to particular stator and rotor pole arc values of the electromagnetic structure [12]. For each couple of pole arcs, outer stator diameter, stack length, airgap length and shaft diameter were fixed dimensions ; the other parameters (rotor radius,

determine curves of intrinsic minimal torque ripple (peak-to-peak value divided by average value) versus average torque and speed with limited copper losses (taking into account real current waveform) and limited "silicon apparent power". The optimum waveforms depend, in fact, both on speed, because of the voltage and current limits of the converter, and on torque because of the magnetic saturation of the motor. A comparison of results allows us to comprehend the compromise necessary to have a reluctance motor-converter set with low torque ripple possibilities. Finally, we examined the validity of the classical hypothesis of non-magnetic coupling between phases. For this, we computed, by the finite-element method, the electromagnetic torque when the three phases are supplied by optimised current waveforms at low speed (weak overlaps of phase currents) and at medium speed (relatively large overlaps).

2/ Optimisation of geometrical dimensions of the various structures

Geometric parameters of doubly-salient variable reluctance motor structure

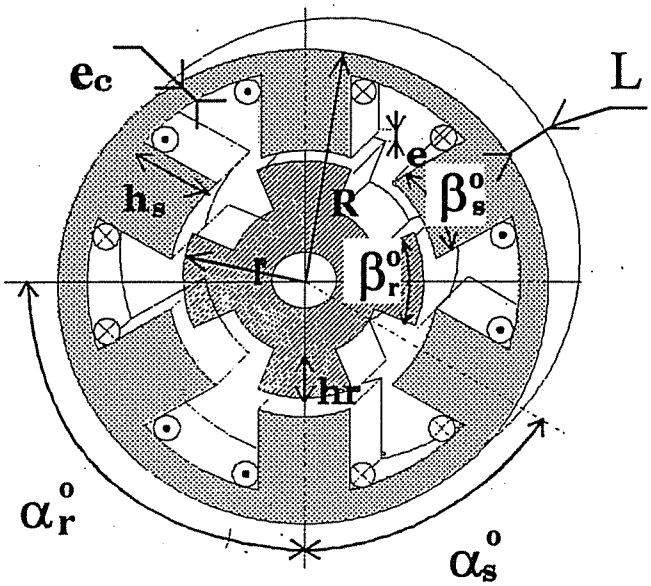

Main geometric parameters of doubly-salient structure

Figure 1

The main geometric parameters are defined in Figure 1. They are :

external sizes :

- L : stack length (fixed value : L = 150 mm)
- R : outer radius (fixed value : R = 125 mm)

stator sizes :

- N_S : number of stator teeth (here : N_S = 6)
- β_S : relative angle of stator teeth :

$$\beta_S = \frac{\beta_S^0}{\frac{2\pi}{N_S}} \qquad (2.1)$$

- e_c : stator yoke thickness
- h_S : height of stator teeth
- e : airgap length (fixed value : 0.8mm)

rotor sizes :

- r: rotor radius
- N_R : number of rotor teeth (here : N_R = 4)
- β_R : relative angle of rotor teeth :

$$\beta_R = \frac{\beta_R^0}{\frac{2\pi}{N_R}} \qquad (2.2).$$

- h_R: height of rotor teeth
- d_a: shaft diameter

Moreover, we define :

- kc : stator yoke coefficient :

$$k_c = \frac{e_c}{\frac{\pi . r}{N_S} . \beta_S} \qquad (2.3)$$

- $$k_r = \frac{r}{R} \qquad (2.4)$$

When N_S, N_R, R, d_a and e are fixed, only parameters k_c k_r, β_R and β_S are variable ; other geometric parameters can easily computed by formulae (2.1) to (2.4).

Computation of average torque and copper losses: Initially, we determined optimum geometric parameters for several couples of relative tooth angle values (β_R and β_S). This optimisation is based on an ideal feeding with square current waveform (current being regulated at constant value between opposition and conjunction positions). Then, the converted energy per stroke W could be computed by the knowledge of flux curves in unaligned and aligned positions (see Figure 2).

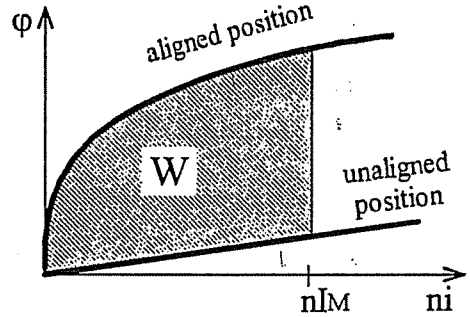

Converted energy per stroke with square current waveform feeding

Figure 2

The polyphase average torque can be computed as :

$$< T >= q . \frac{N_R}{2.\pi} . W \qquad (2.5)$$

where q is the phase number, in this case : q = 3.

Thanks to this simple method, we could optimise very quickly the main dimensions of motor structures. In practice, the copper losses corresponding to these ideal current waveforms are a little smaller than the losses obtained with optimum current waveforms with respect to the torque ripple [8].

Unaligned flux curves can be computed from the results of numerical finite-element analysis [15], where only r, β_S, β_R and hr parameters are influential. Aligned flux curves can be determined by a circuit-type modeling (see Figure 3), where resistances represent saturable reluctances [11]. Magnetic characteristics of the laminations are given in Figure 4.

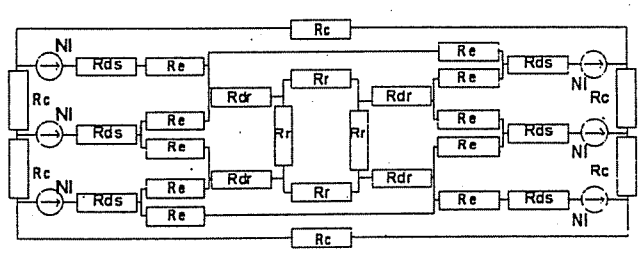

Equivalent magnetic circuit in aligned position

Figure 3

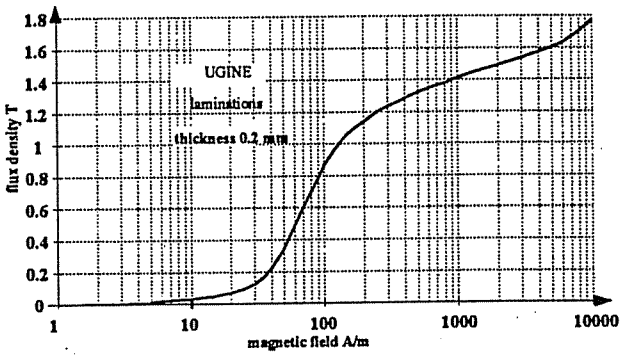

Magnetic characteristics of laminations

Figure 4

Copper losses can be computed from the knowledge of the rms values of phase currents and resistance values of windings. The winding resistance depends [10] on geometrical parameters (winding cross area), filling factor kb (2.6), the length of the medium turn and copper resistivity at operating temperature ($\rho = 2.2\ 10^{-8}$).

$$k_b = \frac{S_{cu}}{S_b} \tag{2.6}$$

where S_{cu} is the copper area for a stator tooth and S_b is the winding cross area.

$$Sb = hs.\frac{1-\beta s}{2}\ \frac{2\pi.r}{Ns} \tag{2.7}$$

$$Sb \approx \left[1-kr(1+kc.\beta s.\frac{\pi}{Ns})\right](1-\beta s).kr.\frac{\pi}{Ns}.R^2 \tag{2.8}$$

Typically, we can obtain for kb a value of 0.6. Let k_i be the form factor of the current waveform :

$$ki = \frac{nIM}{nIeff} \tag{2.9}$$

In the case of the ideal square wave current : $ki = \sqrt{2}$.
Copper losses P_{cu} can be computed by the equation :

$$P_{cu} = \rho.\frac{N_s}{2}.kl.L.\frac{nIM^2}{ki^2.kb.Sb} \tag{2.10}$$

where kl is a coefficient greater than 1 and equal to the ratio of the medium turn length on two times the stack length (2.L). This coefficient allows taking into account the length of turn ends.

Geometric parameter optimisation results: We computed the average torque of each machine for constant copper losses and then for approximately constant heating. We optimised k_c and k_r parameters for each couple of (β_R , β_S) values. Figures 5a and 5b show the influences of β_S, kr and kc on average torque with constant copper losses (1500 W) and a copper resistivity of $2.2\ 10^{-8}\ \Omega.m$. Rotor pole arc has a lower sensitivity. We can see that optimum values for kr and kc exist.

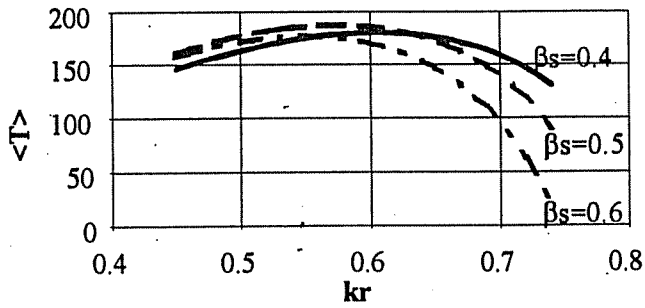

Average torque versus kr and β_S (parameter)
β_R = 0.5, kc = 1.1, P_{cu} = 1500 W

Figure 5a

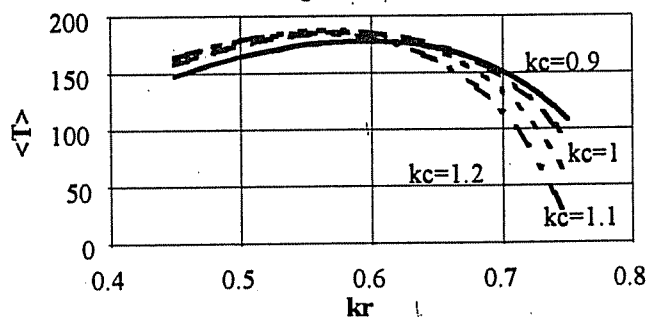

Average torque versus kr and kc = 1.1 (parameter)
β_R = 0.5, β_S = 0.6, P_{cu} = 1500 W

Figure 5b

Table 1 sums up the principal optimal parameters for each studied machine M1 to M5. Values of β_R and β_S are chosen inside the "feasible triangle" [1]. The minimum value of β_S that provides a minimum overlap of single-phase torque waveforms is equal to 0.5 (β_S^0 = 30°). Rotor pole arc β_R^0 is always greater than stator pole arc β_S^0.

N° machine	β_s	β_r	k_c	k_r
M1	0.7 (42°)	0.5 (45°)	1.04	0.54
M2	0.6 (36°)	0.45 (40.5°)	1.06	0.56
M3	0.6	0.5	1.06	0.56
M4	0.6	0.55 (49.5)	1.06	0.56
M5	0.5 (30°)	0.5	1.08	0.58

Computed structures and their principal parameters

Table 1

Figure 6 shows cross-sections of machine structures M1, M2 and M4.

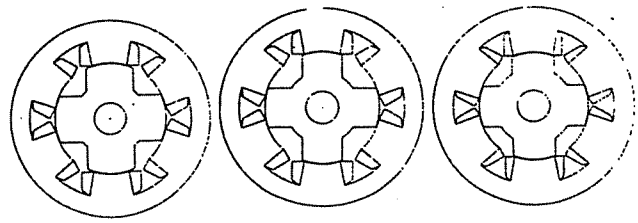

M1 M2 M4

Machine structures M1 (β_s = 0.7, β_r = 0.5), M2 (β_s = 0.6, β_r = 0.45) and M4 (β_s = 0.6, β_r = 0.55)

Figure 6

3/ Torque and Flux curve computation by Finite-Element Method:

With a software package (Maxwell 2D), we computed magnetic characteristics φ (ni, θ) and T (ni, θ) for each machine M1 to M5 (θ is the electric angle, θ = 0 corresponds to the unaligned position). Figure 7 shows flux arrays. In Figure 8, we can see the major impact of β_S values on the angular duration of torque production [16, 17]. Low values of β_r give "flat" flux and torque in the opposition zone, and high values give "flat" flux and torque in the conjunction zone.

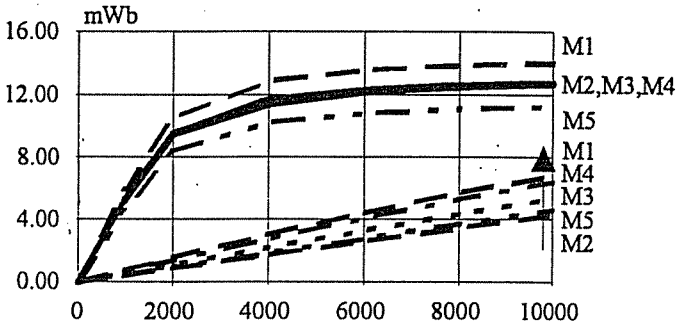

Flux characteristics in unaligned and aligned positions for M1 to M5

Figure 7

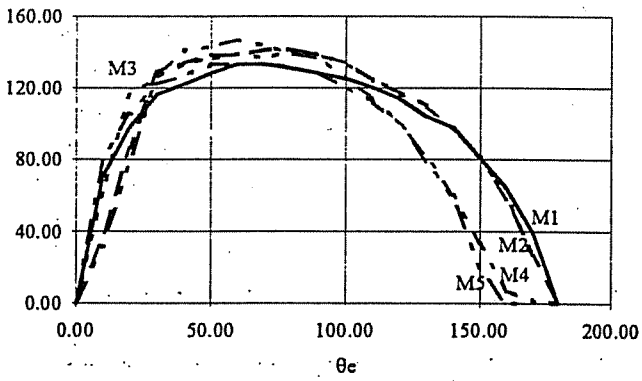

Torque waveforms for M1 to M5 at nIM = 10 000 A

Figure 7

4 OPTIMISATION OF CURRENT WAVEFORMS TO MINIMISE TORQUE RIPPLE

To minimise the torque ripple, we optimised current waveforms to obtain single-phase trapezoidal torque waveforms with two angle parameters A1 and A2 (angle overlap) as defined in Figure 9.

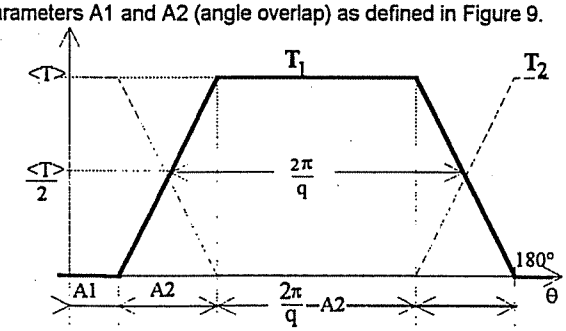

Torque reference waveform

Figure 9

By use of T(ni, θ), we can determine the current or amperes-turns waveform corresponding to the torque reference waveform. Then, by characteristic φ (ni, θ), we can compute the voltage required to obtain the previous current. So, we optimised A1 and A2 angles to minimise copper losses. Because of the non-linear characteristics of the variable reluctance motor, A1 and A2 optimum values depend on the torque reference level.

"Apparent silicon power" limitation: When the speed increases, required voltage reaches high values greater than the DC voltage which supplies the converter-motor set. To minimise the cost of the converter, we determine the turn number of the phase windings to have a "converter sizing factor" fd equal to about 10 (identical to the one obtained in the case of an alternative current motor supplied by a three-phase inverter). The "converter sizing factor" [7] is defined as :

$$f_d = \frac{n_k . U_{kM} . I_{kM}}{P_{max}} \qquad (3.1)$$

where nk is the semi-conductor switch (transistor-diode sets) number and U_{kM} and I_{kM} are the maximum voltage and current constraints applied to the switches. With an asymmetrical half-bridge converter (6 switches for a three-phase motor), we can write :

$$f_d = 2.\frac{U_{kM} . I_{kM}}{P/q} \qquad (3.2)$$

Then, it is sufficient to analyse each phase independently by limiting the product $U_{kM}.I_{kM}$ to a value equal to :

$$U_{kM} . I_{kM} = \frac{U_{kM}}{n} . nI_{kM} = \frac{f_d}{2} . \frac{P}{q} \qquad (3.3)$$

If fd = 10, then : $U_{kM} . I_{kM} = 5.\frac{P}{q}$. The turn number will be determined, for each machine, in order to obtain maximum power under a given DC voltage. The maximum "apparent silicon power" is independent of the turn number because :

$$[U_{kM} . I_{kM}]_{max} = \left[\frac{U_{kM}}{n} . nI_{kM}\right]_{max} \qquad (3.4)$$

For a 6/4 three-phase structure with a maximum power of 31 kW ((100 N.m à 3000 rpm) and with a maximum value of amperes-turns equal to 8000 A, the maximum voltage per turn is limited to : 5,63 V.

Because of the limited voltage, it is not possible to supply the motor with optimum current waveform at high torque and/or high speed. So, the torque ripple cannot equal zero. Then, we optimised A1 and A2 angles to minimise the torque ripple with respect to torque reference level and to speed. Figure 10 shows an example of computed waveforms of reference torque, the corresponding theoretical current, the voltage with limitation, distorted current and distorted torque (because of voltage limitation).

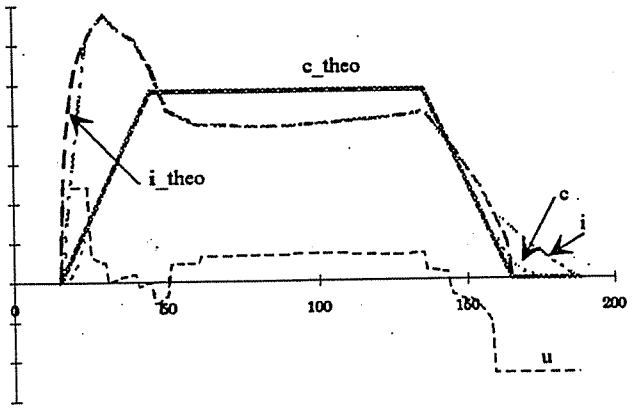

Computed waveforms
of theoretical (without voltage limitation) torque and current
and "real" (with limitation) torque, current and voltage
Figure 10

When several couples (A1, A2) yield to the same torque ripple, we chose the couple which gave minimum copper losses.

Results of current waveform optimisation for each machine: For each machine, we computed, with limited "silicon apparent power", the minimum torque ripple versus speed and torque. Figure 11 shows the curve array of the ratio of peak-to-peak torque ripple to average torque for machine M1. We can notice increasing torque ripple with increasing speed and torque. In this case, it is intrinsically impossible to obtain a constant instantaneous torque at average torque greater than 40 N.m. For a base speed of 3,000 rpm, peak-to-peak torque ripple reaches 20% at an operating point 100 N.m, 1,500 rpm. When speed increases, voltage reaches its maximum (limit of the DC supply) on a large range of the angular period. At base speed, feeding is in full wave voltage mode. Beyond base speed, the switched reluctance motor is fed by square-wave voltage and the operating point is regulated by the adjustment of control angles (advance and magnetisation). So, the SRM can provide maximum power on an extended range of speed.

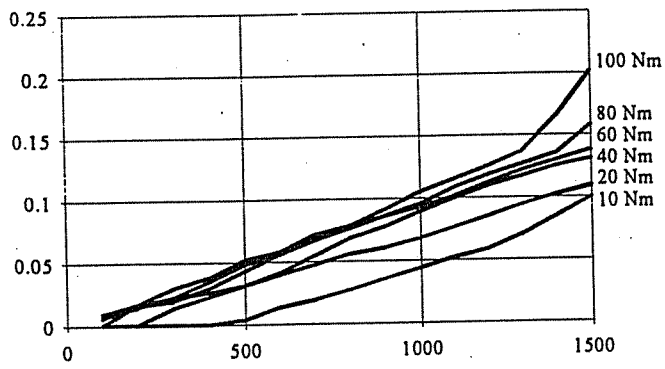

Minimum peak-to-peak torque ripple (relative value to average torque)
versus speed and torque
Figure 11

To compare the different machines, Figures 12 and 13 show minimum torque ripple (relative peak-to-peak) and copper losses (taking account of real winding cross-area and turn ends) versus speed for a torque of 90 N.m, respectively. We can notice the favourable effect of increasing stator pole arc to reduce torque ripple (increasing angular range of production of torque) [8] and its unfavourable result on copper losses because of reduction of winding area. It is clear that a design compromise between torque ripple and copper losses exists. Effects of rotor pole arc is clear too. Increasing of rotor pole arc increases the conjunction angular zone in which the permeance is constant. Then an optimal value of β_r exists to obtain a compromise between angular duration requiered to switch on the current (during opposition zone) and angular duration requiered to switch off current (during conjunction zone) [12].

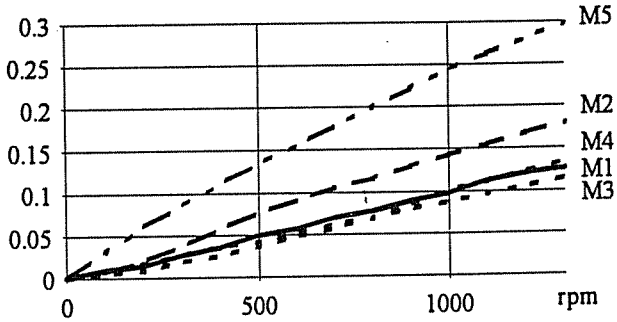

Minimum ripple torque versus speed for the various machines
(<T> = 90 N.m)
Figure 12

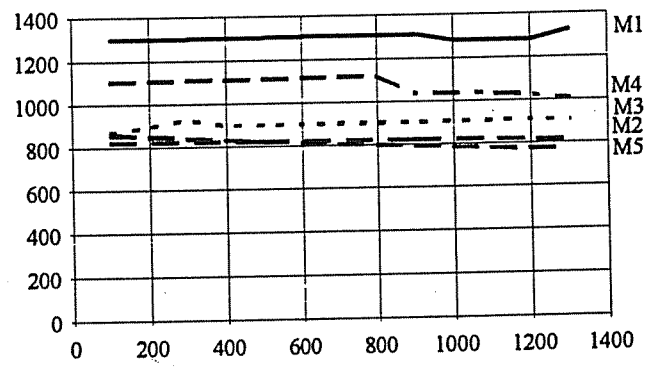

Copper losses versus speed at minimum torque ripple
(<T> = 90 N.m)
Figure 13

5. CONCLUSIONS

In this paper, we tried to optimise electromagnetic structure and current waveforms of a switched reluctance motor to minimise torque ripple. To reduce computation time at acceptable values, we proceeded step by step. The most important parameters of the electromagnetic structure of an SRM are pole arcs. At first, we optimised the main dimensions of 5 machines which all have the same outer size and same copper losses. Then, we computed their torque characteristics and their optimum current waveforms to minimise torque ripple with constrained "silicon apparent power". We saw that a design compromise, on stator pole arc in terms of torque ripple and copper losses, exits. Influence of the rotor pole arc is less significant than the stator pole arc but an optimal value exists. A motor, with dimensions near those presented in this article, has been designed, built and tested. For confidentiality reasons, we are not able to give the corresponding results. But, we are able to confirm

the validity of our computations, particularly, by the finite-element method, and the magnetic model of the laminations were also valid.

6. REFERENCES

[1] P.J. LAWRENSON, J.M. STEPHENSON, P.T. BLENKINSOP, J. CORDA, N.N. FULTON
"Variable-Speed Switched Reluctance Motors".
Proceedings IEE, Vol. 127, Pt. B, No. 4, July 1980, pp.253-265.

[2] D.P. TORMEY, D.A. TORREY
"The Design of a Low-Current Variable-Reluctance-Motor Drive with Constrained Torque Ripple".
ICEM 90, Vol.3, pp.788-793.

[3] R.S. WALLACE, D.G. TAYLOR
"Three Phase Switched Reluctance Motor Design to Reduce Torque Ripple".
ICEM 90, Vol.3, pp.783-787.

[4] J. CORDA, S. MASIC, I. BAKALAR, N. SELJUBAC
"Effects of the Form of Magnetic Circuits on Torque Pulsations of Switched Reluctance Motor".
ICEM 90, Vol.I, pp.88-93.

[5] R.S. WALLACE, D.G. TAYLOR
"Low Torque Ripple Switched Reluctance Motors for Direct Drive Robotics".
IEEE Trans. on Robotics and Aut. Vol.7, N°6, Dec.91, pp.733-742.

[6] D.S. SCHRAMM, B.W. WILLIAMS, T.C. GREEN
"Torque Ripple Reduction of Switched Reluctance Motors by Phase Current Optimal Profiling"
PESC 92, pp.857-860.

[7] B. MULTON, C. GLAIZE
"Size Power Ratio Optimization for the Converters of Switched Reluctance Motors".
IMACS'TC1, Nancy, September 1990, pp.325-331.

[8] J.-Y. LE CHENADEC
"Minimization of Torque Ripple of Switched Reluctance Motors. Influence of Magnetic Characacteristic of Machine and of Inverter Limits" (in French). Ph. D. Thesis, 28 April 1993, ENS Cachan.

[9] J.Y. LE CHENADEC, B. MULTON, S. HASSINE
"Current Feeding of Switched Reluctance Motor. Optimization of the Current Waveform to Minimize the Torque Ripple", IMACS TC1'93, Montréal, 7-9 July 1993.

[10] B. MULTON, C. JACQUES
"Comparison of Performances of Two Self-Commutated Electric Motors : the Permanent Magnet Brushless DC Motor and the Switched Reluctance Motor", Conf. Clean Vehicles, La Rochelle (France), 15-19 novembre 1993, pp.295-302.

[11] M. GEOFFROY
"Etude de l'influence des paramètres géométriques du circuit magnétique sur les formes d'onde de perméance et de couple des machines cylindriques à réluctance variable à double saillance",
Thesis PARIS XI - E.N.S. de CACHAN, January 1993.

[12] B. MULTON, S. HASSINE, J.Y. LE CHENADEC
"Pole Arcs Optimization of Vernier Reluctance Motors Supplied with Square Wave Current".
"Electric Machines and Power Systems", Vol.21, N°6, 1993, pp.695-709.

[13] H. CAILLEUX, B. LE PIOUFLE, B. MULTON, C. SOL
"A Precise Analysis of the Phase Commutation for the Torque Non-Linear Control of a Switched Reluctance Motor. Torque Ripples Minimization"
IEEE Conf. IECON'93, Hawaï, Dec. 1993, pp.1985-1990..

[14] M. GEOFFROY, B. MULTON, E. HOANG, R. NEJI
"Couplage de méthodes pour le calcul rapide des caractéristiques électromagnétiques des machines à réluctance variable à double saillance", Colloque "méthodes informatiques de la conception industrielle", ESIM Marseille, 18 juin 1993, pp.81-90.

[15] D.P. TORMEY, D.A. TORREY, P.L. LEVIN
"Minimum Airgap-Permeance Data for the Doubly-Slotted Pole Structures Common in Variable-Reluctance-Motors". proc. IEEE, Seattle Sept. 1990, pp.196-200.

[16] A.R. EASTHAM, H. YUAN, G.E. DAWSON, P.C. CHOUDHURY, P.M. CUSACK
"A Finite Element Evaluation of Pole Shaping in Switched Reluctance Motor".
Electrosoft, 1990, Vol.1, N°1, pp.55-67.

[17] M. MOALLEM, C.M. ONG, L.E. UNNEWEHR
"Effect of Rotor Profiles on the Torque of a Switched Reluctance Motor".
Proc. IAS, Seatle 90, pp.247-253./ IEEE Trans. I.A. Vol.28, N°2 March/April 92, pp.364-369.